Numerical Modelling Of Navigable Rivers: Influence Of Navigation Structures In The Meuse River Flow.

A. R. Patil
Belgian Nuclear Research Center & Université catholique de Louvain, Institute of Mechanics, Material and Civil Engineering, Mol, Belgium

J. Lambrechts, I. Draoui
Université catholique de Louvain, Institute of Mechanics, Materials and Civil Engineering, Louvain-la-Neuve, Belgium.

F. Fiengo Perez
Belgian Nuclear Research Center, Mol, Belgium

E. Deleersnijder
Université catholique de Louvain, Institute of Mechanics, Materials and Civil Engineering & Earth and Life Institute, Louvain-la-Neuve, Belgium

ABSTRACT: The numerical simulation of navigable rivers is a complex task due to the functioning of hydraulic structures that introduces alterations in the river flow dynamics. Therefore modules for simulation of hydraulic works such as weirs and underflow gates have been included in the finite element, discontinuous Galerkin SLIM modelling framework. In this study we evaluate the simulation capabilities of the new version of SLIM for representing the hydrodynamics of the highly regulated rivers. The case study selected for this evaluation is the Meuse River, in Belgium. The flow simulations were compared against measurements done along the Meuse River. The evaluation results shows Nash–Sutcliffe Efficiencies around 0.68 and 0.92 for water level and discharge respectively. Although, a good agreement for discharge was obtained, slightly lower efficiencies were observed for water levels. The main reason for this deviation are lack of information regarding operation rules.

1 INTRODUCTION

Numerical modelling of river hydraulics involves the representation of different complex dynamic mechanisms. Moreover, many rivers are regulated or subjected to the operation of hydraulic structures to divert, rise or store the water. The representation of the functioning of such hydraulic structures in numerical models requires specific assumptions. The presence of these structures introduces a discontinuity in the flow, which is difficult to deal with during the solution of the hydrodynamic equations. Therefore, the most common approach to represent the influence of these structures is to incorporate stage-discharge relationships into the numerical scheme. As a reference example, DHI's Mike replaces the momentum by the energy equation at the location of the structure (Mike 11 Reference Manual 2017). This is a standard approach when using finite difference methods. On the other hand when finite volumes and discontinuous finite element schemes are used, an alternative approach can be followed, where special fluxes are applied at the location of the structures.

Independently of the approach followed, the application to a real case scenario can bring its own challenges. The stage-discharge relationships are derived from scaled-physical models developed in laboratories and determined mostly under steady state conditions. The derived relationships include a set of equations corresponding to different possible flow regimes. Unfortunately, during the operation, the real structure will work under flow conditions that considerably deviate from those used during the laboratory setup. Moreover, these equations provide criteria for identification of flow regimes (limits between regimes) and the selection of the corresponding formulation. The implementation of these structures in numerical models demands additional considerations. For example, it is appreciated that, when flow conditions are very close to the limits between two flow regimes, instabilities occur. Therefore, besides a robust numerical scheme, an accurate representation of inter-regime flow conditions and a correct estimation of the flow over the structure are required.

The abovementioned methods are applied to the Meuse River, which is 905 km long and stretches across three countries. It originates in France, flows through Belgium and The Netherlands to reach the North Sea. The water flowing in Belgium (covering 152 km distance) is highly controlled by hydraulic structures. The primary objective of these structures is to prevent urban dwelling from flooding and to provide assistance in navigation. In the first context, several studies have been conducted to assess the effects of floods in the Meuse River basin (Beckers et al. 2013 & Tu et al. 2005). These studies include hydrological modelling (Leander et al. 2005) of the catchment, impact of climate change on flow (de Wit et al. 2001), groundwater flow and transport (Batlle-Aguilar et al. 2016). Although effort has been done in simulating the hydrodynamics of the Meuse River (Beckers et al. 2013) the influence of hydraulic structures was not fully addressed in the studies mentioned above. The operation of hydraulic works can have a significant influence on water levels and on the propagation of water wave due to sudden changes in the operation of the structure under both high and low flow regimes.

Here we focus, on the evaluation of the accuracy of the flow simulations in the Belgian Meuse River by taking into account the influences of existing hydraulic structures on the hydrodynamics under different flow regimes. To this aim, additional modules for the simulation of hydraulic structures were incorporated in the discontinuous Gakerkin method of the SLIM modelling framework (Second generation Louvain-la-Neuve ice ocean model, www.slim-ocean.be). The main advantage of SLIM is its capacity to deal with abrupt water level changes induced by the operation of structures, owing to its discontinuous formulation.

2 MEUSE RIVER SYSTEM

The Meuse River flows through France and Belgium and then reaches the north sea through the Netherlands as shown in Figure 2. The Belgium part of the Meuse River is highly regulated by a combination of weir systems and lock chambers which play a major role in the river flow dynamics. The Meuse River is split in different segments bounded by weirs. The function of the weirs is to rise the water level to obtain a sufficient hull for navigation. Right beside each weir, a lock chamber is placed that assists the movement of vessels between segments. Downstream of the city Liège the Meuse River splits into two branches, one of them flows to the North and feeds the Albert Canal and Flemish navigation network. The second branch flows into the Netherlands following the natural course of the Dutch Meuse. The diversion is controlled by a weir located at Monsin (Liège). Later, the Dutch Meuse splits further into three branches; the natural Dutch Meuse, the Juliana canal and the Zuid-Willemsvaart canal.

3 NUMERICAL MODELLING: IMPLEMENTATION OF HYDRAULIC STRUCTURES

To represent the flow dynamics in the river domain, it is customary to use the one-dimensional Saint-Venant equations (Szymkiewicz 2010), which read:

$$\frac{\partial}{\partial t}\begin{bmatrix} A \\ Q \end{bmatrix} + \frac{\partial}{\partial x}\begin{bmatrix} Q \\ \frac{Q^2}{A} + \frac{P}{\rho} \end{bmatrix} = \begin{bmatrix} 0 \\ gA\frac{dh}{dx} - gs + \frac{F}{\rho} \end{bmatrix} \quad (1)$$

where Q and A represent the volumetric flow rate and the cross-sectional area; t is the time and x is the along-flow coordinate. The solution of Saint-Venant equations by means of the discontinuous Galerkin (DG) method starts with the division of the domain in discrete elements where Q and A are approximated as follows:

$$U = [Q \quad A]^T \qquad F(U) = \left[Q \quad \frac{Q^2}{A} + \frac{P}{\rho}\right]^T \qquad S(U) = \left[0 \quad gA\frac{dh}{dx} - gs + \frac{F}{\rho}\right]^T \quad (2)$$

where U represents the vector of variables, F is the vector of fluxes and S represents the source term vector. In the framework of the DG method, U is approximated using a set of independent linear shape functions with the unknown nodal values as shown below:

$$U|_{\Omega_e} \simeq U_h|_{\Omega_e} = \sum_{i=1}^{2} \phi_i U_i^e \quad (3)$$

The solution is obtained by transforming Equation 1 into a weak formulation within an element:

$$\int_{\Omega_e} \frac{\partial U}{\partial t} \phi_i dx - \int_{\Omega_e} F.\nabla\varphi_i dx + [F\varphi_i]_{x_e}^{x_{e+1}} = \int_{\Omega_e} S\varphi_i dx \quad (4)$$

The advantage of this approximation is that the connection between the element edges is discontinuous (Figure 1) and in the boundary term $[F\varphi_i]_{x_e}^{x_{e+1}}$ the flux needs to be computed in order to connect each element. One such technique is the Riemann Problem to compute a discontinuity at a single point. The Riemann problem considers the left and right conditions at the point and provides a solution for the characteristic curves based on the eigenvalues of the Jacobian matrix in the region of the point under consideration (Toro 2009). This technique applied to numerical methods is used to derive the equation for the flux at the point (star region) of discontinuity. However, in the context of a numerical scheme the solution for the Riemann problem has to be approximated. Several methods for approximating the solution exist. Accordingly the following equation is used to compute the flux:

$$\begin{cases} on\ \Omega_e\ A^*\left(-\frac{Q_0}{A_0}+\sqrt{\frac{gA_0}{b^*}}\right)+Q^* = A_2^e\left(-\frac{Q_0}{A_0}+\sqrt{\frac{gA_0}{b^*}}\right)+Q_2^e \\ on\ \Omega_{e+1}\ A^*\left(-\frac{Q_0}{A_0}+\sqrt{\frac{gA_0}{b^*}}\right)-Q^* = A_1^e\left(-\frac{Q_0}{A_0}+\sqrt{\frac{gA_0}{b^*}}\right)+Q_1^{e+1} \end{cases} \quad (5)$$

where U^* is computed from the volume flux conservation, Q^* from left and right elements and subsequently the flux is calculated as a function of U^* ($F(U^*)$). Details about the implementation of the DG method and the Riemann solver for Saint Venant equations can be found in Draoui et al. 2020. For the implementation of the hydraulic structure into the DG Method, a discontinuity at the location of the structure is imposed. At this point, unlike the discontinuity between elements where the Riemann solver is used , the equation to calculate the flux is replaced based on the stage discharge relationship of the structure as shown in Figure 1. In this figure the edges are represented by circles and nodes around the discontinuity at the structure by a triangle. At this point, the discharge through the structure is calculated and corresponding positive flux is assigned to the right node and negative flux to the left in the context of the DG Method.

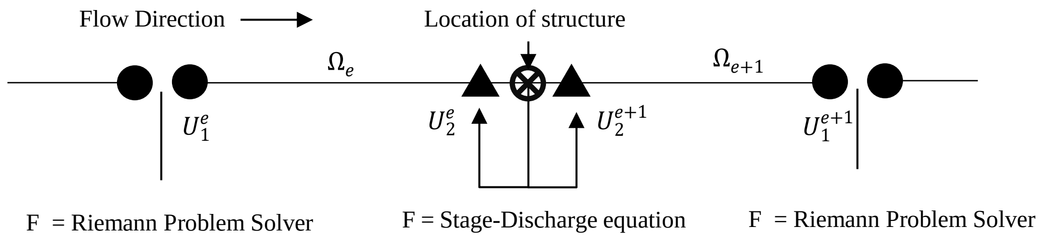

Figure 1: Representation of the nodes in DG Method and the treatment of flux by stage-discharge relationships for the imposed discontinuity at the location of hydraulic structure.

3.1 *Calculation of Discharge for weirs*

The discharges over the weir are calculated as functions of the water levels upstream and downstream of the structure. Under these conditions, two scenarios can arise. In the first one, the downstream water level is sufficiently lower that it does not affect the upstream flow conditions (free flow condition) and in the second case, the downstream water level is sufficiently high to influence the upstream discharge and water level (Submerged Flow Conditions). The equation for weirs is as follows (Bos 1976):

$$Q = \begin{cases} C_1 W(H_{us}-H_w)\sqrt{(H_{us}-H_w)} \quad for \quad \frac{(H_{ds}-H_w)}{H_{us}} < \frac{2}{3}\ Free\ flow \\ C_2 W(H_{ds}-H_w)\sqrt{(H_{us}-H_{ds})} \quad for \quad \frac{(H_{ds}-H_w)}{H_{us}} \geq \frac{2}{3}\ Submerged\ flow \end{cases} \quad (6)$$

where H_{ds} = water level downstream; H_{us} = water level upstream; h_w = level of the weir crest; C = weir coefficient; and W = width of the structure.

3.2 *Calculation of Discharge for Underflow gates*

For the underflow gates the discharge is also calculated from the upstream and downstream water level. The relevant equations are:

$$Q = CWB\sqrt{2gH} \tag{7}$$

$$H = H_{us} - H_{ds} \tag{8}$$

where, B = gate opening height.

4 MODEL SETUP OF THE MEUSE RIVER

For the extraction of cross sections of the Meuse River, a combination of bathymetric and topography data was used to have a complete representation of the cross section that includes the river bed elevations and flood plains. The elevation data for both models were collected by ‘Service public de Wallonie’. The bathymetry data in the river was measured using multi beam sonars and echo sounders in certain shallow water with a resolution of 10 cm and the topography was measured using the airborne LiDAR technique for a resolution of 1m. The position of the river banks was defined from ortho-photos. The spacing between the extraction of cross sections is 500 meters. The Manning coefficient for the river was chosen as 0.033 $sm^{-1/3}$, which is in the range for coarse sand and gravel bed (Arcement and Schineider 1989). The structure dimensions in the Meuse River were defined based on on-site measurements.

Discharge at boundaries were prescribed as follows: at the beginning of the Meuse River in Belgium with Chooz Measurement station, the Sambre river with Ronet and Ourthe river with Sauhied (Figure 2). The other tributaries are considered as point sources. For the downstream boundaries, the water levels at Kanne located in Albert Canal and Lixhe located in the Meuse River were applied (Figure 2). The time series used for the boundary conditions and point sources were obtained from “Service public de Wallonie”.

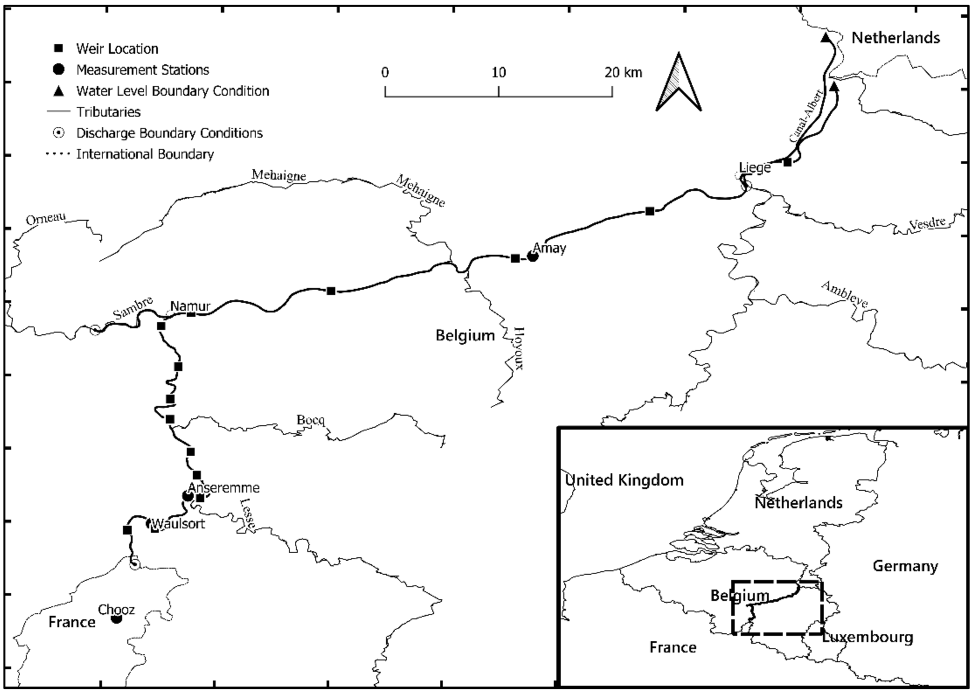

Figure 2: Map of the section of Meuse River flowing through Belgium: The location of measurement stations used, boundary conditions and location of the weirs in the river stream

The internal water distribution between Albert Canal and the Meuse River, is regulated by the weir located near Liège in Monsin. This weir operates to keep a constant water level in Albert Canal (around 60m TAW) and to divert a minimum discharge to the Netherlands. The influence of the lock chambers placed along the Meuse River is neglected. This is because they have a local influence and their operation is not continuous and largely depends on schedule of the navigation traffic.

5 RESULTS AND DISCUSSION

The accuracy of the model was evaluated by comparing the model simulations with the measurements of water level and discharges recorded by the gauging stations located along the river. The Nash –Sutcliffe Efficiency (NSE) criterion was used for this evaluation. Although the NSE criterion shows a good agreement between observation and simulations, an additional accuracy measure is required to establish the prediction capabilities of SLIM. Here we complement our results with a 95% probability confidence interval in order to define the errors associated to the water level and discharge simulations. During the model evaluation, sudden changes in the water level were observed as a consequence of the structure operation. Based on the magnitude of the water level shifts observed in the measurement data, the operation rules of the weirs were defined and incorporated in the model . The combination of the operation rules and the stage-discharge relationships allowed us to consider the elevation changes in the weir crest during the calculation of the discharge. Though there are several stations installed along the Meuse and its tributaries, the majority record the water levels and only few of them measure the discharge. This situation largely limits the model verification of mass conservation.

In this results section, we compare the model simulations against the measurement data of two discharge and one water level stations. Mostly, the water levels are constantly monitored upstream of the place where the weir is located to guide the operation of the structure. According to the water level data at these points, the water flow through the different segments of the Meuse River depends only on the upstream conditions. The difference between the upstream and downstream water levels at the weir location is sufficiently large to avoid the influence of the back water effect on the flow over the structure. Hence, we take advantage of this situation and we adopt a segment based calibration approach. On the other hand, the reduced number of river flow stations and the distance between them, makes it difficult to define the water inflows, such as the runoff from the inter-catchment and flash flooding, coming from the urban zones during rain events. Moreover, the water extraction can only be estimated from publications due to the lack of information about daily and hourly withdrawals.

5.1 *Model Calibration*

The measurement data of water flow at Waulsort and the water levels at Anseremme were chosen for the calibration of the model. The distance along the river between both stations is approximately 7 km. During the calibration, the value of the weir coefficient is set constant for all flow regimes.

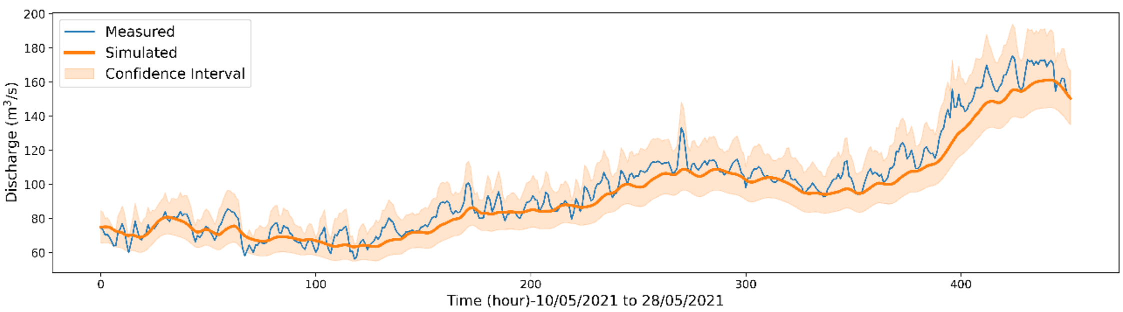

Figure 3: Waulsort discharge station: comparison of simulated and measured values with confidence interval for calibration.

The above figure shows a comparison of the simulated and measured discharges at Waulsort. It also contains 95% confidence interval for the entire period. For the discharge measurement at Waulsort, a NSE coefficient equal to 0.94 is achieved and the confidence interval covers 99% of the total simulated data. It is observed that the model simulation closely follows the main trend of the observation time series. However, it does not catch the fluctuations along the mean flow. Among the possible reasons, this behavior can be mentioned by the influence of navigation on the measurements. Vessels disrupt the water level and propagate waves while displacing. This situation could certainly introduce uncertainties in the measurements.

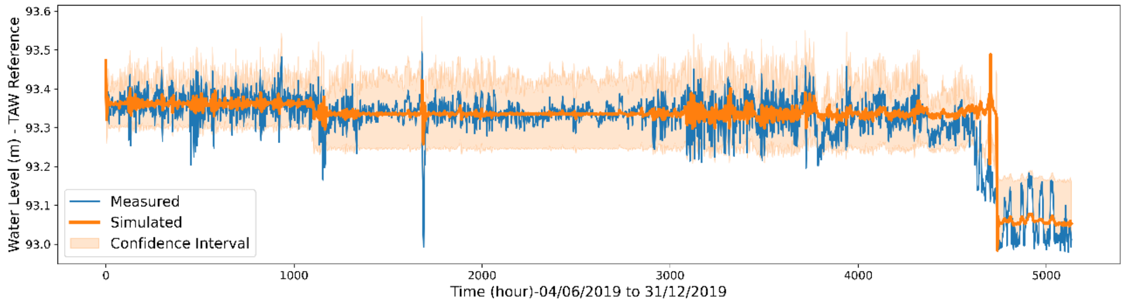

Figure 4: Anseremme water level station: comparison of simulated and measured values with confidence interval for calibration.

From the water level measurements, it can be seen (Figure 4) that the influence of the weir operation is evident. These abrupt changes in the water levels can be reproduced with the help of the operation rules derived during the model set up. Figure 4 shows a comparison of the water level between the measurement station at Anseremme and the simulated values. An NSE coefficient of 0.74 and a confidence interval with coverage of 96% is achieved. The oscillations observed in the measurements have a mean amplitudes of approximately 10 cm. Again, the model is capable of predicting the main trend of the time series but not the oscillations. As in the case of the discharge time series discussed before, it is presumed that waves induced by navigation and wind could be responsible for this oscillations.

5.2 *Meuse River Model: Validation*

For the validation of the Meuse River model the data for Anseremme station is now considered for one year period of 01/01/2018 to 31/12/2018 which is different from the calibration period.

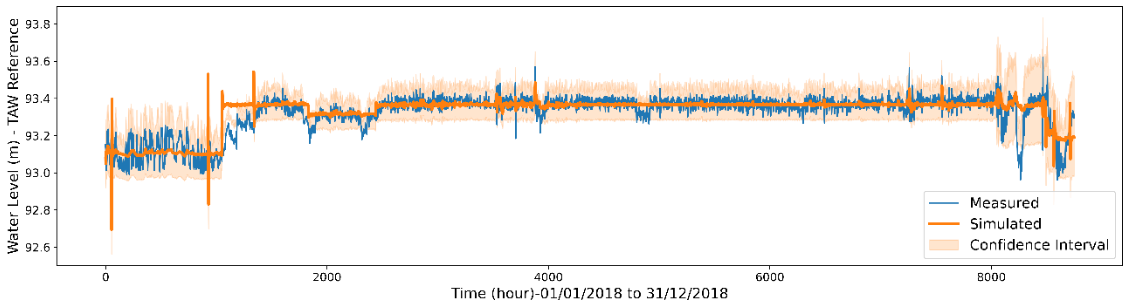

Figure 5: Anseremme water level station: comparison of simulated and measured values with confidence interval for validation.

The comparison of water levels between the model and measured values has an NSE coefficient of 0.68 and 95 % of the simulations are covered by the confidence interval (Figure 5). The lower value in NSE coefficient in comparison to that obtained during calibration can be justified by the fact that the length of the time series used for validation is longer. During this period, it was observed that the flow over weirs corresponds mainly to free flow conditions.

In the entire Meuse River network, only Chooz and Amay stations have substantial measurement data for discharge. Hence, Amay is the only suitable station for the validation of flow rate. The comparison between the simulated and measured discharges for Amay station is shown below:

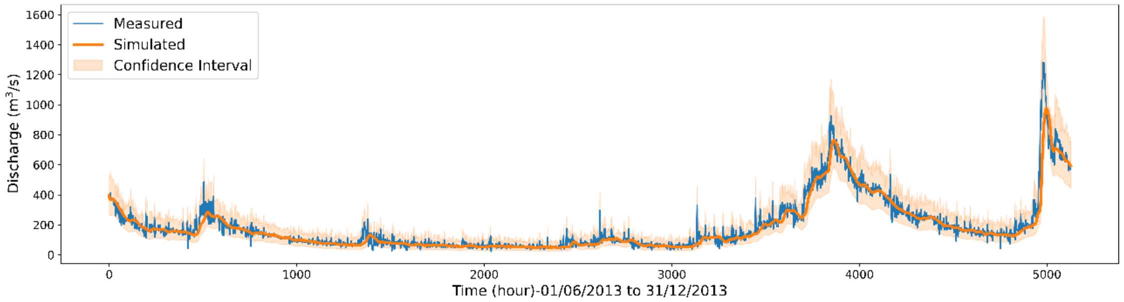

Figure 6: Amay water level station: comparison of simulated and measured values with confidence interval for validation.

A NSE coefficient of 0.92, a cumulative deficit equal to 4.3 % and coverage of 98 % was obtained (Figure 6). These show a high degree of agreement in the simulation with the measured flow. However, differences can be seen for some discharge peaks. The primary reasons for this are the inflows discharged into the river during high precipitation, not only from the Meuse River inter-catchment but also from the tributaries not included in the model and the sewage systems from cities.

6 CONCLUSION AND RECOMMENDATIONS

The simulations provided by the SLIM model are in agreement with the measurements of water level and discharges. The SLIM model is capable of representing the flow trends and the water levels. Though the fluctuations are not captured, it does not necessarily mean that the accuracy of the model is limited. But, it points out that other physical phenomena such as wind friction and waves induced by vessels could also influence the flow dynamics. These phenomena could also explain the oscillations observed in the measured data. Moreover, the confidence interval shows that some water inflows are not considered. The lack of discharge measurement stations makes it difficult to estimate correctly the lateral inflow rate during rainfall events due to surface runoff coming from the sides of the river, point discharge flash flood originated in urban areas and small streams. The flash floods and the contribution of small streams could explain the reason why the model underestimates the peaks during high flows. Regarding water levels, the new model for the representation of hydraulic works has proved to be useful when simulating water levels. The combination of stage-discharge relationship and operation rules makes it possible not only to match the average water levels but to reproduce the sudden shifts of water level induced by the operation of the structures. Based on the results obtained after calibration and validation, we are confident that SLIM is a suitable tool for the optimization of complex operation schemes of hydraulic structures aimed for flood control. Additionally, SLIM can be coupled to a water quality module for the simulation of the fate and transport of pollutants in rivers where the flow is largely influenced by regulating structures.

The uncertainties in the source term can be reduced if hydrological models are used for the simulation of rainfall-runoff. This would facilitate the estimation of the lateral inflow and the point sources along the rivers. Additionally, further studies are required to determine the contribution of the wind and navigation induced waves to oscillations registered by the water level stations.

REFERENCES

Arcement, G., Schineider, V., 1989. Guide for selecting Manning's roughness coefficients for natural channels and flood plains.

Batlle-Aguilar, J., Orban, P., Dassargues, A., Brouyère, S., Carabin, G., 2016. Identification of groundwater quality trends in a chalky aquifer threatened by intensive agriculture, Hydrogeology Journal.

Beckers, A., Dewals, B., Erpicum, S., Dujardin, S., Detrembleur, S., Teller, J., Pirotton, M., Archambeau, P., 2013. Contribution of land use changes to future flood damage along the river Meuse in the Walloon region. Natural Hazards and Earth System Sciences 13, 2301–2318.

Bos, M.G., 1976. Discharge measurement structures, International Institue for land reclamation and improvement. International Institute for land Reclamation and Improvement, Wageningen, The Netherlands.

de Wit, M.J.M., Warmerdam, P.M.M., Torfs, P.J.J.F., Uijlenhoet, R., Roulin, E., Cheymol, A., van Deursen, W.P.A., van Walsum, P.E. v, Ververs, M., Kwadijk, J.C.J., Buiteveld, H., 2001. Effect of climate change on the hydrology of the river Meuse.

Draoui, I., Lambrechts, J., Legat, V., Sandra, Hoitink, T., Deleersnijder, E., 2020. Discontinuous Galerkin method for 1D river flows. River Flow 2020 - Proceedings of the 10th Conference on Fluvial Hydraulics 1114–1121.

Leander, R., Buishand, A., Aalders, P., de Wit, M., 2005. Estimation of extreme floods of the River Meuse using a stochastic weather generator and a rainfall-runoff model. Hydrological Sciences Journal 50, 1089–1103.

Mike 11 Reference Manual, 2017. A Modelling System for Rivers and Channels Reference Manual.

Szymkiewicz, R., 2010. Numerical Modeling in Open Channel Hydraulics. Water Science and Technology Library 83.

Toro, E.F., 2009. Riemann solvers and numerical methods for fluid dynamics: A practical introduction. Riemann Solvers and Numerical Methods for Fluid Dynamics: A Practical Introduction 1–724.

Tu, M., Hall, M.J., de Laat, P.J.M., de Wit, M.J.M., 2005. Extreme floods in the Meuse river over the past century: aggravated by land-use changes? Physics and Chemistry of the Earth, Parts A/B/C 30, 267–276.